Journal of Bioenergetics and Biomembranes, Vol. 37, No. 5, October 2005 (© 2005)
DOI: 10.1007/s10863-005-8639-0

Kinetic Evidence for the Uniport Mechanism Hypothesis in the Mitochondrial Tricarboxylate Transport System

A. De Palma,[1] G. Prezioso,[1] and V. Scalera[2,3]

Received July 29, 2005; accepted September 1, 2005

The kinetics of the transport of citrate by the tricarboxylate transport system located in the inner mitochondrial membrane was studied in proteoliposomes containing the purified carrier protein, in order to verify the previously hypothesized mechanism of uniport (J. Bioenerg. Biomembr. 35, 133–140, 2003) and achieve some information on the kinetic properties of the carrier transport system. For this purpose, a mathematical model has been elaborated and the experimental data were analyzed according to it. The results indicate that the data actually fit with the uniport model, and hence it is confirmed that the carrier has a single binding site for its substrates and can oscillate between the inside and outside form, in both the free and substrate-bound states. The rearrangement of the free form is slower than the bound form in both directions. The dissociation constants for the internal substrate are at least one order of magnitude higher than the one for external citrate. As a consequence of these last two points, the rate of citrate transport by the carrier is much higher when it operates in exchange with another substrate than when it operates in net uniport.

KEY WORDS: Mitochondria; proteoliposomes; tricarboxylate carrier; citrate transport; kinetics; uniport.

INTRODUCTION

Among the carrier proteins present in the inner membrane of rat liver mitochondria, the tricarboxylate transport system plays an important role in fatty acid synthesis, gluconeogenesis, and the transfer of reducing equivalents across the membrane. This carrier, in fact, catalyzes the efflux of citrate, together with a proton, from the matrix in an electroneutral exchange for another tricarboxylate-H^+, malate, or phosphoenolpyruvate (Bisaccia *et al*., 1993).The tricarboxylate carrier protein has been isolated and reconstituted into liposomes in a functionally active state (Bisaccia *et al*., 1989, 1990; Kaplan *et al*., 1990). As in the case of majority of the mitochondrial metabolite carriers (Kaplan, 2001), the citrate carrier has been proposed to function according to a sequential reaction mechanism (Bisaccia *et al*., 1993), which implies that one internal and one external substrate molecule form a ternary complex with the carrier protein. Recently, however, we have formulated an alternative hypothesis for the transport mechanism of uniport, based on the observation of a unidirectional efflux of citrate by proteoliposomes specifically catalysed by the carrier (De Palma *et al*., 2003).

The aim of this study was to perform a kinetic characterization of the transport process, in order to gain further experimental support for this hypothesis, as well as to achieve a more detailed description of the transport mechanism.

MATERIALS AND METHODS

Materials

Hydroxyapatite (Bio-Gel HTP) and Bio-Beads SM-2 were purchased from Bio Rad, Celite 535 was from Roth, Sephadex G-75 from Pharmacia, [1,5-^{14}C]citrate

[1] Dipartimento Farmaco-biologico, Università degli Studi di Bari, Bari, Italy.
[2] Dipartimento di Fisiologia Generale ed Ambientale, Università degli Studi di Bari, Bari, Italy.
[3] To whom correspondence should be addressed at Dipartimento di Fisiologia Generale ed Ambientale, Università degli Studi di Bari, via Amendola 165/A, 70126 Bari, Italy; e-mail: v.scalera@biologia.uniba.it.

from Amersham International (Amersham, UK), egg-yolk phospholipids (L-α-phosphatidylcholine from fresh turkey egg yolk), 1,4-piperazinediethanesulphonic acid (Pipes), cardiolipin, Triton X-114, and Triton X-100 were from Sigma. All other reagents were of analytical grade purity.

Purification and Reconstitution of the Tricarboxylate Carrier

The tricarboxylate carrier was purified from rat liver mitochondria as previously described (Bisaccia *et al*., 1989). The purified protein was reconstituted into liposomes by the removal of detergent with a hydrophobic column (Palmieri *et al*., 1995). In this procedure, the mixed micelles containing detergent, protein, and phospholipids were repeatedly passed through the same Amberlite XAD column. The composition of the initial mixture used for reconstitution was 200 μL of purified protein in 0.5% Triton X-100 (about 0.1 μg protein), 90 μL of 10% Triton X-114, 100 μL of 10% egg yolk phospholipids in the form of sonicated liposomes prepared as described earlier (Dulley and Grieve, 1975), citrate or other substrates at the concentrations indicated in the figure legends, and 20 mM Pipes pH 7 in a volume of 700 μL. After vortexing, this mixture was passed 24 times through the same Bio-Beads SM-2 column (0.5 cm$\times$3.6 cm) pre-equilibrated with the same buffer and the substrate at the same concentration of the starting mixture. All the operations were performed at 4°C, except the passages through Bio-Beads SM-2 column that were performed at room temperature.

Transport Measurements

The external substrate was removed from reconstituted proteoliposomes by chromatography at 4°C on a Sephadex G-75 column (0.7 $\times$ 15 cm) pre-equilibrated with 50 mM NaCl, 10 mM Pipes at pH 7.0. The transport activity was determined by measuring the influx or the efflux of labelled substrate in exchange for unlabeled substrate. For efflux exchange measurements, the proteoliposomes containing 10 mM internal citrate were prelabelled by carrier-mediated exchange equilibration. This was achieved by incubating the proteoliposomes with 0.1 mM [^{14}C]citrate at high specific radioactivity for 30 min at 25°C. After this incubation time, the external radioactivity was removed by passing the proteoliposomes through a Sephadex G-75 column as described above. Transport at 25°C was started by adding [^{14}C]citrate to the proteoliposomes (influx) or unlabelled citrate (efflux) to the prelabelled proteoliposomes, as indicated in the figure legends of each experiment. In the uptake experiments (influx), transport was stopped by adding 20 mM pyridoxal 5′-phosphate. In the case of efflux, transport was terminated by addition of a mixture of 38 mM pyridoxal 5-phosphate and 10 mM 1,4-dithioerythritol. In both cases, in control samples the inhibitors were added at time zero according to the inhibitor-stop method (Palmieri *et al*., 1995). In order to remove the external substrate, each sample of proteoliposomes (100 μL) was transferred to the Sephadex G-75 column (0.6 cm$\times$8 cm), eluted with 1.3 mL of 50 mM NaCl and collected in 4 mL of scintillation mixture, vortexed and counted (Palmieri *et al*., 1995). In influx kinetic measurements, the initial transport rate was calculated from the radioactivity taken up by the proteoliposomes. In the case of efflux, the rate was calculated from the difference between the radioactivity measured at time zero and that measured after the incubation. Transport is always expressed as mmol/min per gram of protein.

Each experiment was performed at least three times, always giving qualitatively similar results. All experimental data reported are the average of triplicate assays. Error bars were omitted as they were generally lower than the height of the symbols and anyway never exceed 5% of the mean.

Protein Determination

Protein was determined by the Lowry method modified for the presence of nonionic detergents (Bisaccia *et al*., 1985).

RESULTS

Premise

A kinetic study of the transport process catalyzed by the proteoliposome incorporated tricarboxylate carrier protein, has been performed by analyzing exchange-influx and exchange-efflux rates of substrate transport. A radio-labelled substrate ([^{14}C]-citrate) was present in the external medium, in the former case, and inside the liposomes in the latter, in the presence of a cold counter-substrate.

The proposed uniport mechanism for the transport process can be described by a sequence of steps as, in the following scheme, for the influx of labelled citrate (A^*) against internal cold citrate (A) or another

substrate (B):

$$\begin{array}{rrl} A^*_e + C_e \rightleftarrows CA^*_e & \text{fast :} & K_{Ae} \\ CA^*_e \rightarrow CA^*_i & \text{slow :} & k_2 \\ CA^*_i \rightleftarrows C_i + A^*_i & \text{fast :} & K_{Ai} \\ \multicolumn{3}{c}{\text{but also :}} \\ C_e \rightarrow C_i & \text{slow :} & k_3 \\ \multicolumn{3}{c}{\text{as inward steps. Then :}} \\ C_i + A_i \rightleftarrows CA_i & \text{fast :} & K_{Ai} \\ CA_i \rightarrow CA_e & \text{slow :} & k_{-2} \\ CA_e \rightleftarrows C_e + A_e & \text{fast :} & K_{Ae} \\ \multicolumn{3}{c}{\text{or}} \\ C_i + B_i \rightleftarrows CB_i & \text{fast :} & K_{Bi} \\ CB_i \rightarrow CB_e & \text{slow :} & k_{-4} \\ CB_e \rightleftarrows C_e + B_e & \text{fast :} & K_{Be} \\ \multicolumn{3}{c}{\text{but also :}} \\ C_i \rightarrow C_e & \text{slow :} & k_{-3} \\ \multicolumn{3}{c}{\text{as outward steps.}} \end{array} \tag{1}$$

In this scheme, we use the reasonable assumption of a "rapid equilibrium" steady state, where the interactions among substrates and carrier are considered as fast steps to reach equilibrium, while the steps of rearrangement of the various forms of the carrier inside the membrane are considered slow and, therefore, rate limiting. Velocity equations for influx and efflux have been obtained by adapting the Haldane procedure of enzyme kinetics (Segel, 1975) to the membrane transport process described in the scheme. With the assumption of rapid equilibrium, the equilibrium constants

$$\begin{aligned} K_{Ae} &= \frac{[A_e][C_e]}{[C\,A_e]} \quad K_{Ai} = \frac{[A_i][C_i]}{[C\,A_i]} \\ K_{Be} &= \frac{[B_e][C_i]}{[C\,B_e]} \quad K_{Bi} = \frac{[B_i][C_i]}{[C\,B_i]} \end{aligned} \tag{2}$$

regulate the substrate-carrier interactions, while the kinetics constants K regulate the respective slow rearrangement steps.

Our aim was to verify whether experimental data fit to such a model.

The presence of a stationary state condition is an experimental data, since the measured transport rates in any case remain constant for easily measurable times. As long as the stationary state condition holds, the concentrations of the various forms of the carrier (see Scheme (1)) are constant, with the consequence that

$$\begin{aligned} &k_2[C\,A_e] + k_4[C\,B_e] + k_3[C_e] \\ &\quad = k_{-2}[C\,A_i] + k_{-4}[C\,B_i] + k_{-3}[C_i] \end{aligned} \tag{3}$$

On the other hand, we also have

$$\begin{aligned} C_T = {} &[C_e] + [C_i] + [C\,A_e] \\ &+ [C\,A_i] + [C\,B_e] + [C\,B_i] \end{aligned} \tag{4}$$

where C_T is the total concentration of the carrier molecule (generally expressed as pmol/mg protein or similar).

By means of Eqs. (2)–(4), the concentration of each form of the carrier can be expressed as a function of the concentrations of the substrates present, as it is shown for the cases treated.

We have firstly analyzed the exchange between external and internal molecules of citrate.

Citrate/Citrate Exchange: Influx

Influx experiments were performed by loading proteoliposomes with various concentrations of cold citrate (as described in the Methods section) and then incubating them in media containing variable concentrations of labelled citrate.

In this case, according to the uniport model, we were actually following the step of the transport process regulated by kinetic constant k_2 in Scheme (1). The rate of influx is then expressed by the equation

$$v = k_2[C\,A_e] \tag{5}$$

By making $[CA_e]$explicit from Eqs. (3) and (4), produces the following:

$$\begin{aligned} \vec{v} = {} & k_2 C_T \times [k_{-2}A_iA_e + k_{-3}K_{Ai}A_e]/[(k_{-2} + k_2)A_iA_e \\ & + (k_{-3} + k_2)K_{Ai}A_e + (k_{-2} + k_3)K_{Ae}A_i \\ & + (k_{-3} + k_3)K_{Ai}K_{Ae}] \end{aligned} \tag{6}$$

where the independent variables A_e and A_i are present (indicating, in a simplified form, $[A_e]$ and $[A_i]$) as well as the kinetic and equilibrium constants described in Scheme (1).

Figure 1(A) shows the result of a typical two-substrate experiment, where the rate of influx of externally added labelled citrate was measured. The substrate was present at different external concentrations, and had internal citrate as counter-substrate, also at different concentrations. If external citrate concentration (A_e) was established as the independent variable, a curve was obtained at each internal citrate concentration A_i. These curves fit to hyperbolic saturation equations of the "Michaelis-Menten" type, with the transport rate expressed by

$$\vec{v} = \vec{V}_M \frac{A_e}{A_e + \vec{K}_M} \tag{7}$$

where the parameters V_M and K_M depend on the internal citrate concentration A_i, that is different for each experimental curve.

Double reciprocal plots of the data gave a group of straight lines (Fig. 1(B)), from which kinetic parameters

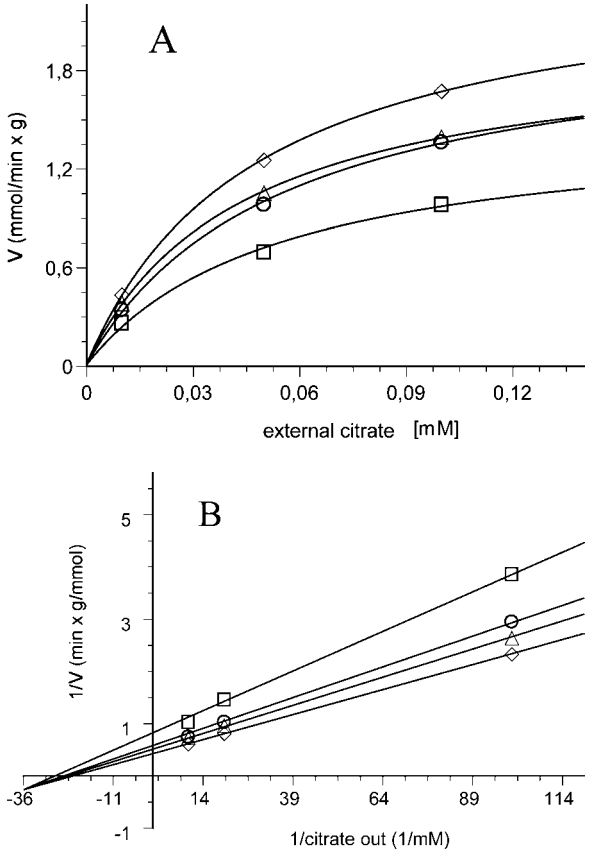

Fig. 1. Two-substrate analysis of the influx of citrate in the presence of internal citrate, catalyzed by the reconstituted tricarboxylate carrier. Dependence of the rate of ^{14}[C]citrate uptake in proteoliposomes on external citrate concentrations (A) and double reciprocal plot showing the dependence of exchange rate on the external concentrations (B). ^{14}[C]Citrate was added at the concentrations of 0.01, 0.05 and 0.1 mM to proteoliposomes containing 3 (□), 6 (◯), 9 (△) and 12 (◇) mM citrate. The rate of uptake is measured in 2 min.

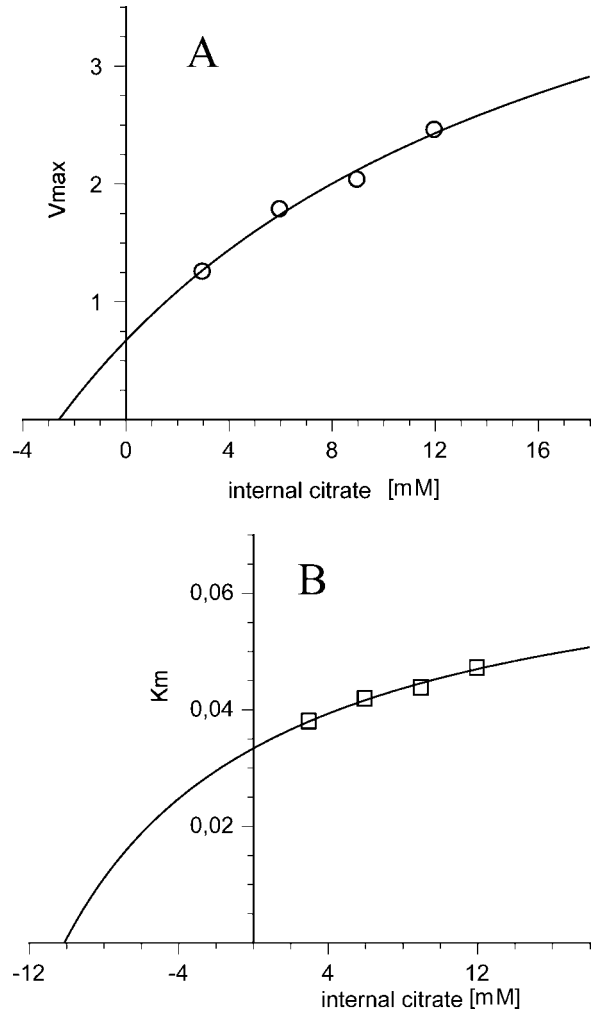

Fig. 2. Second-order plots of the data of Fig. 1. Dependence of the $V_{\max}$ (A) and K_m (B) on the internal citrate concentrations.

can be calculated. It can be observed that these lines, in analogy with two-substrate plots of enzyme kinetics, tend to converge to one point, that is clearly localized in the double negative section of the Cartesian plane. The individuation of the point is achieved by balancing the indications of the fittings independently obtained for the single straight lines in Fig. 1(B). In the experiment shown, the following values are extrapolated for its coordinates: $x_c = -35.6\,\mathrm{mM}^{-1}$, $y_c = -0.27$ mg prot min/nmol. Starting from Eq. (2), it is possible to establish that

$$\vec{x}_c = -\frac{k_2}{k_3}K_{Ae} \quad \vec{y}_c = \left(1 - \frac{k_2}{k_3}\right)\frac{1}{k_2 C_T} \tag{8}$$

If Eq. (6) is applied, keeping A_e as the independent variable and A_i as a parameter, V_M and K_M of Eq. (7) assume the form of functions of A_i as follows:

$$\vec{V}_M = k_2 C_T \frac{k_{-2}A_i + k_{-3}K_{Ai}}{(k_{-2} + k_2)A_i + (k_{-3} + k_2)K_{Ai}} \tag{9}$$

$$\vec{K}_M = \frac{(k_{-2} + k_3)A_i + (k_{-3} + k_3)K_{Ai}}{(k_{-2} + k_2)A_i + (k_{-3} + k_2)K_{Ai}}K_{Ae} \tag{10}$$

Therefore, second-order plots of the parameters V_M and K_M calculated from Fig. 1 should be described by these equations. Actually, Fig. 2 shows that when we plot the extrapolated values of V_M and K_M versus A_i, the points fit to hyperbolic curves not passing through the origin. Such curves can be described by the above equations and can provide numerical values for the parameters therein present, as will be considered in the Discussion section.

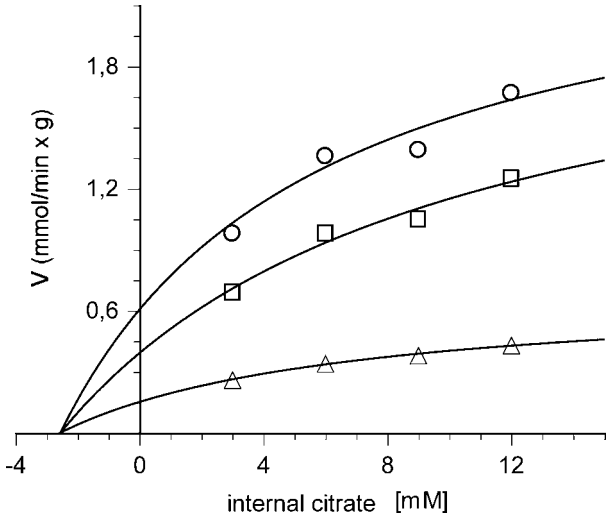

Fig. 3. Replot of data of Fig. 1. Dependence of the rate of citrate uptake in proteoliposomes on internal citrate concentrations. The concentrations of the countersubstrate were as follows: 0.01 (△), 0.05 (□) and 0.1 (◯) mM.

The plot in Fig. 2(A) also allows us to evaluate, by extrapolation, the rate of citrate uptake in the condition of uniport (zero internal citrate concentration), whereas direct measurements in such condition were not possible because the reconstitution of the carrier in proteoliposomes required the presence of a substrate in the reconstitution medium (see also Methods).

The rate of influx of labelled substrate can also be reported versus the internal citrate concentration A_i. In this case, we expect curves showing a hyperbolic saturation with a positive intercept. Indeed, Eq. (6), elaborated by keeping A_e as a parameter, assumes the following form:

$$\vec{v} = \vec{V}_M \frac{A_i + \vec{I}}{A_i + \vec{K}_M} \tag{11}$$

where the parameters V_M and K_M are functions of A_e

$$\vec{V}_M = k_2 C_T \frac{k_{-2} A_e}{(k_{-2} + k_2) A_e + (k_{-2} + k_3) K_{Ae}} \tag{12}$$

$$\vec{K}_M = \frac{(k_{-3} + k_2)\, A_e + (k_{-3} + k_3)\, K_{Ae}}{(k_{-2} + k_2)\, A_e + (k_{-2} + k_3)\, K_{Ae}} K_{Ai} \tag{13}$$

while the parameter I is not

$$\vec{I} = \frac{k_{-3}}{k_{-2}} K_{Ai} \tag{14}$$

and hence represents a common intercept of the curves on the negative side of the abscissa-axis.

The experimental curves in Fig. 3 easily fit to this condition, and allow the calculation of the values for parameters V_M and K_M at each external citrate concentration A_e. Second-order plots for them are shown in Fig. 4. They should fit to the second-order Eqs. (12) and (13). Actually, the data in Fig. 4(A) are compatible with a hyperbolic curve starting from the origin according to Eq. (12), while those in Fig. 4(B) fit to a hyperbolic curve with a positive intercept according to Eq. (13).

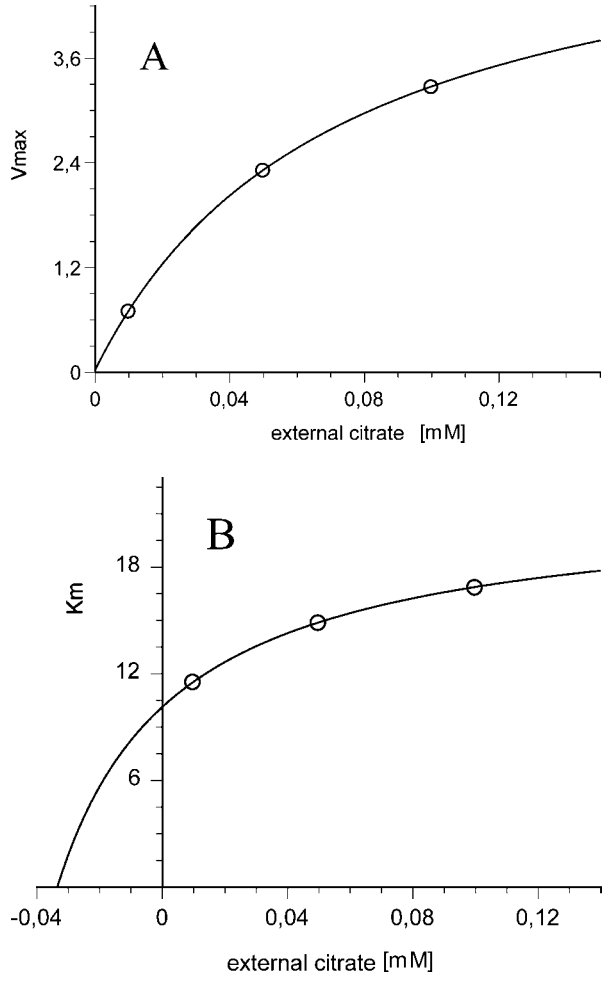

Fig. 4. Second-order plots of the data of Fig. 3. Dependence of the V_{max} (A) and K_M (B) on the external citrate concentrations.

Citrate/Citrate Exchange: Efflux

Efflux experiments were done by loading proteoliposomes with various concentrations of labelled citrate (as described in the Methods section) and then incubating them in media containing variable citrate concentrations. In analogy with influx, the rate of efflux is expressed by

$$v = k_{-2}[C\, A_i] \tag{15}$$

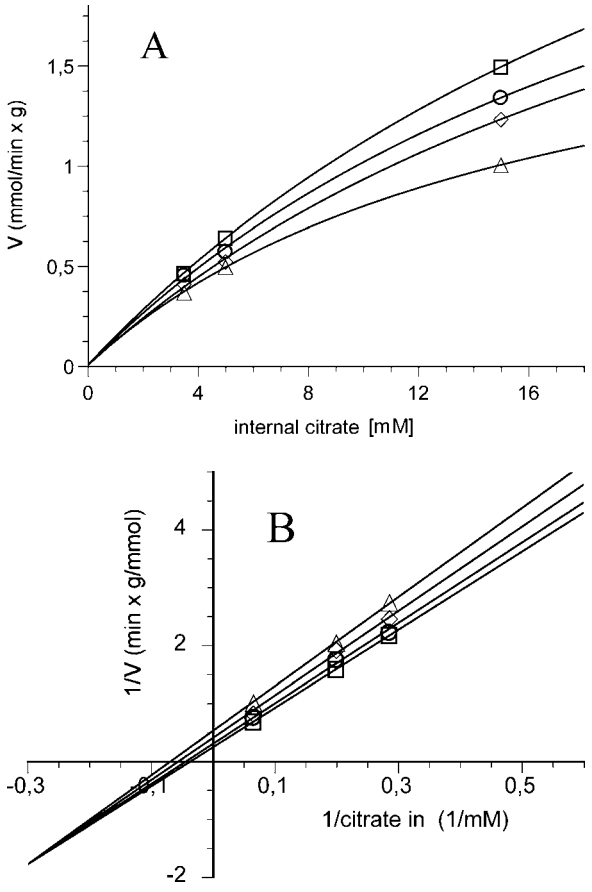

Fig. 5. Two-substrate analysis of the efflux of citrate in the presence of external citrate, catalyzed by the reconstituted tricarboxylate carrier. Dependence of the rate of the ^{14}[C]citrate efflux by proteoliposomes on internal citrate concentrations (A) and double reciprocal plot showing the dependence of efflux rate on the internal concentrations (B). Cold citrate was added at the concentrations of 0.066 (△), 0.1 (◇), 0.2 (◯) and 1 (□) mM to proteoliposomes containing 3.5, 5 and 15 mM citrate. The rate of efflux is measured in 2 min.

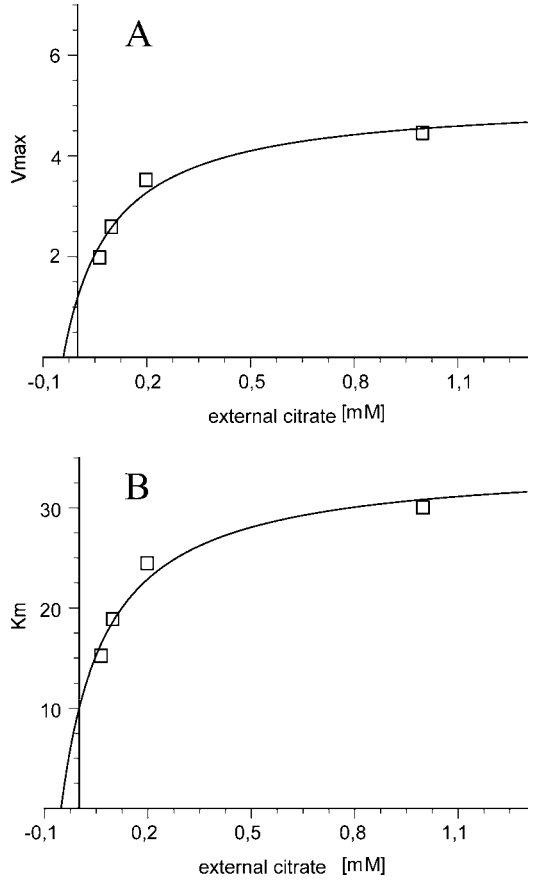

Fig. 6. Second-order plots of the data of Fig. 5. Dependence of the $V_{\max}$ (A) and K_M (B) on the external citrate concentrations.

By making $[CA_i]$ explicit from Eqs. (3) and (4), the following equation is obtained:

$$\overleftarrow{v} = k_{-2}C_T \times [k_2 A_e A_i + k_3 K_{Ae} A_i]/[(k_{-2}+k_2)A_e A_i + (k_{-2}+k_3)K_{Ae}A_i + (k_{-3}+k_2)K_{Ai}A_e + (k_{-3}+k_3)K_{Ae}K_{Ai}] \quad (16)$$

The rates of efflux of labelled citrate measured in two-substrate experiments are reported in Fig. 5 (A) as rate versus internal citrate concentration and in Fig. 5 (B) as double reciprocal plot. In Fig. 5(A), it can be observed that the curves follow a hyperbolic "Michaelian" kinetics, according to the equation

$$\overleftarrow{v} = \overleftarrow{V}_M \frac{A_i}{A_i + \overleftarrow{K}_M} \quad (17)$$

The double reciprocal plot in Fig. 5(B) shows a family of straight lines which tend to converge to a point in the double negative quadrant, in analogy with the influx experiment shown in Fig. 1. In this case, the extrapolated coordinates of the point, expressed by

$$\overleftarrow{x}_c = -\frac{k_{-2}}{k_{-3}}K_{Ai} \quad \overleftarrow{y}_c = \left(1 - \frac{k_{-2}}{k_{-3}}\right)\frac{1}{k_{-2}C_T} \quad (18)$$

are $x_c = -0.3\,\text{mM}^{-1}$, and $y_c = -1.8$ mg prot min/nmol.

Appling Eq. (16) by keeping A_i as the independent variable and A_e as a parameter, V_M and K_M of Eq. (17) assume the form of functions of A_e as follows:

$$\overleftarrow{V}_M = k_{-2}C_T \frac{k_2 A_e + k_3 K_{Ae}}{(k_{-2}+k_2)A_e + (k_{-2}+k_3)K_{Ae}} \quad (19)$$

$$\overleftarrow{K}_M = \frac{(k_{-3}+k_2)A_e + (k_{-3}+k_3)K_{Ae}}{(k_{-2}+k_2)A_e + (k_{-2}+k_3)K_{Ae}}K_{Ai} \quad (20)$$

Again, second-order plots of the parameters V_M and K_M as calculated from Fig. 5 should be described by these equations. As can be observed in Fig. 6 (A) and (B),

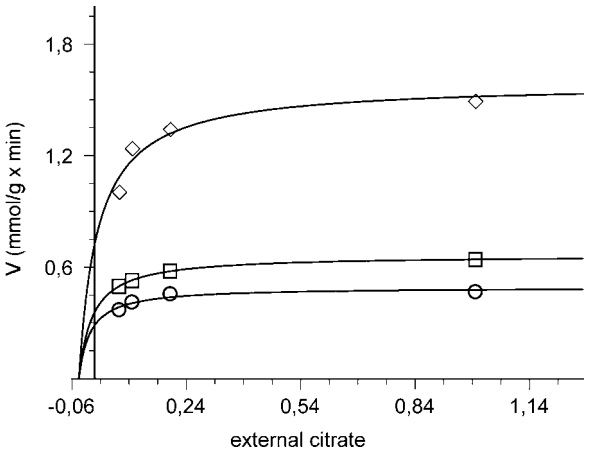

Fig. 7. Replot of data of Fig. 5. Dependence of the rate of citrate efflux by proteoliposomes on the external citrate concentrations. The concentrations of the counter-substrate were as follows: 3.5 (◯), 5 (□), and 15 (◇) mM.

the extrapolated values for V_M and K_M, respectively fit to hyperbolic curves, both having positive intercepts on the ordinate-axis. The intercept in Fig. 5(A) provides a value for the maximal rate of the citrate efflux at zero citrate external concentration, i.e. in the condition of uniport efflux.

When the experimental rates of citrate efflux are plotted against the external citrate concentration, keeping A_i as a parameter, we expect a saturation curve for each value of A_i. The following equation can be obtained from general Eq. (16)

$$\overleftarrow{v} = \overleftarrow{V}_M \frac{A_e + \overleftarrow{I}}{A_e + \overleftarrow{K}_M} \tag{21}$$

which should describe the curves. In this equation, parameters K_M and V_M are functions of A_i

$$\overleftarrow{V}_M = k_{-2} C_T \frac{k_2 A_i}{(k_{-2} + k_2)A_i + (k_{-3} + k_2)K_{Ai}} \tag{22}$$

$$\overleftarrow{K}_M = \frac{(k_{-2} + k_3)A_i + (k_{-3} + k_3)K_{Ai}}{(k_{-2} + k_2)A_i + (k_{-3} + k_2)K_{Ai}} K_{Ae} \tag{23}$$

while I is a constant,

$$\overleftarrow{I} = \frac{k_3}{k_2} K_{Ae} \tag{24}$$

and then represents the common intercept of the curves on the abscissa-axis.

The experimental data reported in Fig. 7 are shown to fit well to this interpretation, allowing an evaluation of I and of the K_M and V_M. Again, Eq. (16) provides an analytical description of the functions K_M and V_M. Equation (22)

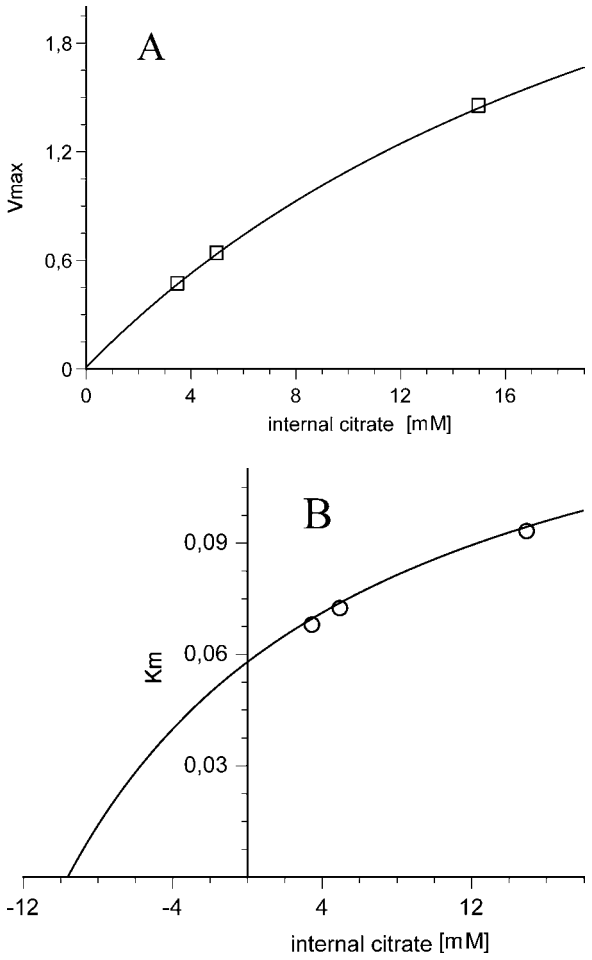

Fig. 8. Second-order plots of the data of Fig. 7. Dependence of the V_{max} (A) and K_M (B) on the internal citrate concentrations.

describes a hyperbole passing through the origin, while Eq. (23) represents a hyperbole with a positive intercept. The second-order plots in Fig. 8 show that the V_M and K_M extrapolated from Fig. 7 fit to Eq. (22) (Fig. 8(A)) and Eq. (23) (Fig. 8(B)), respectively.

Citrate/Malate Exchange: Citrate Uptake

We have evaluated the uptake of labelled external citrate with malate present inside the proteoliposomes. In this case, the general equation for influx assumes the following form:

$$\begin{aligned}\vec{v} = k_2 C_T \times [&k_{-4} B_i A_e + k_{-3} K_{Bi} A_e]/[(k_{-4} + k_2)B_i A_e \\ &+ (k_{-3} + k_2)K_{Bi} A_e + (k_{-4} + k_3)K_{Ae} B_i \\ &+ (k_{-3} + k_3)K_{Bi} K_{Ae}]\end{aligned} \tag{25}$$

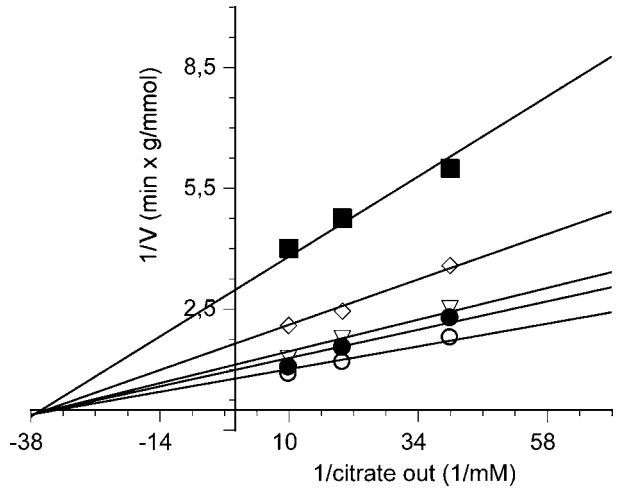

Fig. 9. Two-substrate analysis of the influx of citrate in the presence of internal malate, catalyzed by the reconstituted tricarboxylate carrier. Double reciprocal plot showing the dependence of ^{14}[C]citrate uptake rate, measured in 2 min, on external citrate. ^{14}[C]Citrate was added at the concentrations of 0.025, 0.05 and 0.1 mM to proteoliposomes containing 1.5 (■), 3 (◇), 6 (▽), 9 (●) and 12 (○) mM malate.

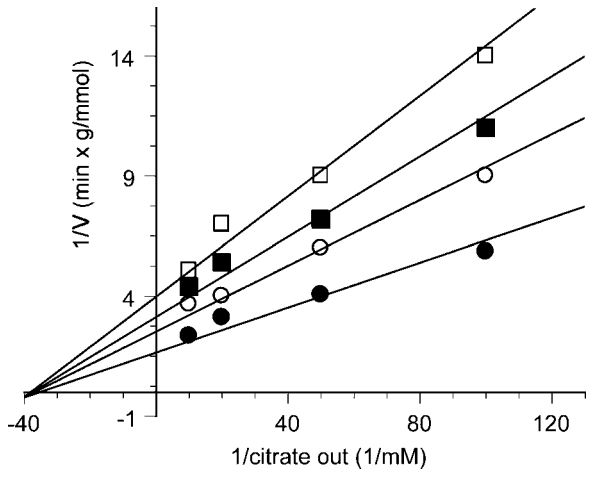

Fig. 10. Two-substrate analysis of the influx of citrate in the presence of internal citrate or internal malate, catalyzed by the reconstituted tricarboxylate carrier. Double reciprocal plot showing the dependence of ^{14}[C]citrate uptake rate, measured in 2 min, on external citrate. ^{14}[C]Citrate was added at the concentrations of 0.01, 0.02, 0.05 and 0.1 mM to proteoliposomes containing 6 (□) and 12 (◯) mM malate and 6 (■) and 12 (●) mM citrate.

where, in comparison to Eq. (16), the internal malate concentration B_i, the equilibrium constant K_{Bi}, and the kinetic constant k_{-4} are present instead of A_i, K_{Ai} and k_{-2}, respectively (see Scheme (1)).

A typical double substrate experiment for labelled citrate influx is shown in Fig. 9 as double reciprocal plot. It can be seen that straight lines tend to meet at a single point having the coordinates $x_c = -37.0\,\text{mM}^{-1}$, and $y_c = -0.12$ mg prot min/nmol.

It is to be noted that, starting from Eq. (25), these coordinates are expressed by two equations identical to those in Eq. (8). It means that the convergence points obtained in experiments of citrate uptake in exchange with any substrate should theoretically be the same. Actually, the coordinates calculated from Figs. 1(B) and 9 are compatible with each other, taking into account that they come from different proteoliposome preparations. In any case, a direct comparison has been done as shown in Fig. 10, where citrate/citrate and citrate/malate exchanges have been performed in one experiment by using the same proteoliposome preparation. It can be observed that the lines referring to internal citrate and the ones referring to internal malate again tend to meet at one point, and that the coordinates extrapolated are similar to those previously cited ($x_c = -40.1\,\text{mM}^{-1}$, $y_c = -0.27$ mg prot min/nmol in the experiment reported). Citrate uptake was also evaluated in double substrate experiments where three "natural" substrates of the tricarboxylate carrier were used as counter-substrates, i. e. phosphoenolpyruvate, isocitrate, and *cis*-aconitate. It has been found that the values are compatible enough with those obtained in the presence of malate and citrate as counter substrate (data not shown).

DISCUSSION AND CONCLUSIONS

The experimental data presented here are consistent with the previously proposed model of uniport exchange (De Palma *et al.*, 2003), according to which the tricarboxylate carrier protein is able to transport citrate and its other substrates in uniport as well as in exchange with a counter-substrate. In fact, from the model proposed, equations were derived that well satisfy the experimental results. This model implies that the carrier has a single binding site for its substrates, which can be alternatively accessible from inside or outside the membrane. Furthermore, the kinetic data allow us to gain an insight to the transport mechanism. In each experiment, the parameters calculated from the primary and secondary plots provide an approximate information about the relative values of the four kinetic constants, as well as about the values of the dissociation constants of the carrier with respect to its substrates. Taking the citrate uptake experiment as an example as described in Figs. 1–4, we can firstly determine that $k_2 > k_3$, $k_{-2} > k_{-3}$, and $k_{-2} > k_3$. In fact, from Eq. (8) the ratio k_2/k_3 must be >1 because y_c is negative (see Fig. 1(B)) and then $k_2 > k_3$. From Fig. 2(A), it can be observed that the extrapolated $(V_M)_{Ai\to\infty}$ is higher than $(V_M)_{Ai=0}$, hence $k_{-2} > k_{-3}$. From the observation that $y_c < (V_M)_{Ai\to\infty}$

and by comparing Eq. (8) for y_c with the expression of $(V_M)_{Ai\to\infty}$ obtained from Eq. (9), we can observe that $k_{-2} > k_3$.

When we use the parameters calculated from Figs. 1 and 2, as defined by Eqs. (8)–(10), we obtain the following ratios between the kinetic constants: $k_2/k_3 = 34$, $k_{-2}/k_{-3} = 15$, $k_{-2}/k_3 = 3.3$, and $k_2/k_{-2} = 10.5$. Furthermore, an approximate value for $K_{Ai} = 36\,\text{mM}$, and $K_{Ae} = 1.05\,\text{mM}$ can be calculated. Equal evaluations from different experiments provide similar results. Nevertheless, apart from the single values obtained for the kinetic and equilibrium constants, the following features were always observed: (1) $k_2 > k_{-2} > k_3 > k_{-3}$, (2) the ratio: k_3/k_{-3} never exceeds 5, (3) k_2 is at least one order of magnitude higher than k_{-3}, and (4) K_{Ai} is always at least one order of magnitude higher than K_{Ae}.

The fact that k_3 and k_{-3} are significantly lower than k_2 and k_{-2} (point 1) means that the carrier is "mobile" in any form, but its ability to rearrange inside the membrane is higher when it is charged with a substrate. These results rule out the possibility of an obligatory exchange with a 1:1 stoichiometry, since in the presented model it would imply that $k_3 = 0$, $k_{-3} = 0$. In such a case, the double reciprocal plots of Figs 1 (B) and 5 (B) would have presented parallel lines. It should also be stressed that under physiological conditions, the carrier operates essentially in exchange, being that substrates are generally present on both sides of the mithocondrial inner membrane.

The affinity of the carrier for citrate, as described by the dissociation constants K_{Ae} and K_{Ai} results to be much lower on the internal side of proteoliposomes with respect to the external (point 4). Furthermore, when a different molecule is present as internal counter-substrate, the affinity of the carrier for it is always quite low (K_{Bi} are of the same order of magnitude of K_{Ai}). The different ability of the carrier protein to bind its substrates on the two sides of the membrane is not in principle unexpected, since it could be simply due to the asymmetry of the carrier molecule. In any case, the fact that the difference of the dissociation constants is very high (at least one order of magnitude) could also be related to the small size of the proteoliposome vesicle, which determines a higher stretch of the internal layer of the membrane with respect to the external and this could cause an unnatural functionality of the protein in that side.

In conclusion, we have produced, for the first time, significant evidence in favor of the uniport model for the mechanism of citrate transport by the tricarboxylate carrier. Indeed, the results of a number of studies conducted in intact mitochondria and with the purified carrier protein reconstituted in proteoliposomes (Bisaccia *et al.*, 1993) were always explained by a sequential random mechanism which brought to an obligatory exchange. Our recent finding that a citrate efflux occurs in the absence of any counter substrate (De Palma *et al.*, 2003) is in contrast with this interpretation, while the uniport exchange model explains it well. In principle, the "double substrate binding site" model does not exclude an additive ability of the carrier to perform a uniport in efflux and/or in influx, but in that case the general velocity equations would be more complex than those reported in the Results section, in particular would not lead to simple "Michaelian" plots and double reciprocal plots would not be linear. Moreover, it must be noted that the data presented and the mechanism proposed in this paper are not in contrast with the experimental results present in the literature, but simply provide a different interpretation for them.

REFERENCES

Bisaccia, F., De Palma, A., Dierks, T., and Palmieri, F. (1993). *Biochim. Biophys. Acta* **1142**, 139–145.

Bisaccia, F., De Palma, A., and Palmieri, F. (1989). *Biochim. Biophys. Acta* **977**, 171–176.

Bisaccia, F., De Palma, A., and Palmieri, F. (1990). *Biochim. Biophys. Acta* **1019**, 250–256.

Bisaccia, F., Indiveri, C., and Palmieri, F. (1985). *Biochim. Biophys. Acta* **810**, 362–369.

De Palma, A., Scalera, V., Bisaccia, F., and Prezioso, G. (2003). *J. Bioenerg. Biomembr.* **35**, 133–140.

Dulley, J. R., and Grieve, P. A. (1975). *Anal. Biochem.* **64**, 136–141.

Kaplan, R. S. (2001). *J. Membr. Biol.* **179**, 165–183.

Kaplan, R. S., Mayor, J. A., Johnston, N., and Oliveira, D. L. (1990). *J. Biol. Chem.* **265**, 13379–13385.

Palmieri, F., Indiveri, C., Bisaccia, F., and Iacobazzi, I. (1995). *Methods Enzymol.* **260**, 349–369.

Segel, I. H. (1975). *Enzime Kinetics*, Wiley, New York.